



Missouri University of Science and Technology  
Scholars' Mine

---

International Specialty Conference on Cold-Formed Steel Structures

(1996) - 13th International Specialty Conference on Cold-Formed Steel Structures

---

Oct 17th, 12:00 AM

## Moment Rotation Behavior for Concrete Filled SHS Column to Composite Beam Connections

J. S. Lee

Young Bonb Kwon

K. S. Woo

Follow this and additional works at: <https://scholarsmine.mst.edu/isccss>

 Part of the [Structural Engineering Commons](#)

---

### Recommended Citation

Lee, J. S.; Kwon, Young Bonb; and Woo, K. S., "Moment Rotation Behavior for Concrete Filled SHS Column to Composite Beam Connections" (1996). *International Specialty Conference on Cold-Formed Steel Structures*. 1.

<https://scholarsmine.mst.edu/isccss/13iccfss/13iccfss-session6/1>

This Article - Conference proceedings is brought to you for free and open access by Scholars' Mine. It has been accepted for inclusion in International Specialty Conference on Cold-Formed Steel Structures by an authorized administrator of Scholars' Mine. This work is protected by U. S. Copyright Law. Unauthorized use including reproduction for redistribution requires the permission of the copyright holder. For more information, please contact [scholarsmine@mst.edu](mailto:scholarsmine@mst.edu).

## MOMENT ROTATION BEHAVIOR FOR CONCRETE FILLED SHS COLUMN TO COMPOSITE BEAM CONNECTIONS

Lee, J.S.<sup>1</sup>, Kwon, Y.B.<sup>2</sup>, and Woo, K.S.<sup>3</sup>

### Abstract

A series of connection tests were carried out to study the behavior of connections between concrete filled Square Hollow Section(SHS) columns and composite W-section beams. The test connections were four different semi-rigid types selected for application to multi-story building frames. The initial flexural rigidities were estimated by different theories and compared with the simple beam. Moment-rotation relations were simulated using a finite element program and a simple power model was proposed to predict the moment-rotation behavior of connections.

### 1 Introduction

In recent years, there has been an increasing trend of using SHS columns in multi-story buildings in spite of the complexity in fabrication of connections. The connections between tubular columns and composite beams may be regarded as semi-rigid. The semi-rigid joints affect the moment distribution and energy dissipation ability of steel framed structures. As a method to enhance the flexural rigidity of the connections, the tubular column can be filled with oncrete which can reduce the column size and as well as increase fire resistance. The behavior of the connections between large tubular columns in-filled with concrete and W-section beams have been investigated by Ji, et al(1989) and Morita, et al(1992).

In this paper, eleven connections of four different types which were composed of SHS columns and composite W-section beams were tested and compared with the numerical results. The initial flexural rigidity of the connections was estimated by classical theory and beam-line theory and compared with a simple beam. The rigidity ratio of the connections were calculated in several ways and those connections have been regarded as semi-rigid for use in the steel frames of the multi-story buildings. The power model for expectation of the moment-rotation behavior of the connections was proposed and proven quite accurate.

### 2 Connection Models

#### 2.1 Test connection types

Beam ends of building frames are generally subjected to negative bending

---

1)Professor, Department of Civil Engineering, Ulsan University, Kyoungham, Korea.

2)Professor, Department of Civil Engineering, Yeungnam University, Kyounghbuk, Korea.

moments. Therefore, the top flange of the W-section beam ends of the SHS column to W-section beam connections transfers tension forces and the bottom flange transfers compression forces to the SHS columns.

In this test series, it is assumed that the tensile forces are partly resisted by the reinforcing bar in the concrete slab which is fully composited through studs and bond stress and the compressive forces are transferred directly to the flange of concrete filled columns. Four different connection types selected for the tests are given in Fig. 1 and the fabrication methods are as follows:

- (1) SDW model : A W-section beam is directly welded to the SHS column flange
- (2) SEB model : An endplate (156x150x9 mm, 6.14x5.91x0.354 in) is welded to the W-section beam end and the endplate is connected to the SHS column flange by high strength bolts.
- (3) SFB model : 2-Fin plates (75x75x6 mm, 2.95x2.95x0.236 in) are bolted to the W-section web and also to the SHS column flange.
- (4) SCB model : A bottom seating cleat angle(150x130x6mm, 5.91x3.45x0.236 in) is bolted to the W-section flange and the SHS column flange.

## 2.2 Test specimen and configuration

The SHS columns selected for the connection test were 200x200x6mm, 200x200x9mm and column length chosen was 600mm(23.6in) which was approximately three times column width to eliminate the affects of global buckling of the column, i.e., it was nominally 200mm(7.87in) square section with a thickness 6mm(0.236in), 9mm(0.354in). The W-section used was 150x100x6x9mm(5.91x3.94x0.236x0.354in) where each numerals indicated depth, width, web thickness, and flange thickness of the section in a series. The thickness of the concrete slab was 120mm(4.72in) and the width was 800mm(31.5in) which was the minimum effective width. The dimensions are given in Table 1 and the geometries of test sections is drawn on Fig. 2.

The test connections were set up in the upside down position with the simple boundary conditions at both ends. The test specimen was loaded on the column end by a 1000-kN capacity actuator as shown on Fig. 2. Three linear displacement transducers were located at the center and two LDTs were posioned at the both sides of the concrete slab as shown in Fig. 2. Two additional LDTs were positioned at the quater points to measure vertical displacements. Two LDTs were placed at the top of the bottom flange and beneath the concrete slab to measure the horizontal deformation of the column flange. Five electric resistance type strain gages were also attached to measure the strains at the reinforcing bars embeded in the concrete slab.

Table 1 Cross Section Dimesions (unit: mm)

Specimen		SHS Section		W-Section				End Plate or Angle			Re-Bar
		H <sub>c</sub>	t <sub>c</sub>	H <sub>b</sub>	B <sub>b</sub>	T <sub>w</sub>	T <sub>f</sub>	H <sub>e</sub>	B <sub>e</sub>	T <sub>e</sub>	
1 <sup>st</sup> s t a g e	SB-001	.	.	150	100	6	9	.	.	.	8 D16@50
	SDW-F11	200	9	150	100	6	9	.	.	.	
	TDW-F11	200	6	150	100	6	9	.	.	.	
	SFB-F11	200	6	150	100	6	9	2Ls75	75	6	
	SCB-F11	200	6	150	100	6	9	Ls 130	150	9	
2 <sup>nd</sup> s t a g e	SB-002	.	.	150	100	6	9	.	.	.	16 D13@50
	SDW-F22	200	6	150	100	6	9	.	.	.	
	SEB-F22	200	6	150	100	6	9	156	150	9	
	SFB-F22	200	6	150	100	6	9	2Ls75	75	6	
	SCB-F22	200	6	150	100	6	9	Ls 130	150	9	
	SDW-F32	200	6	150	100	6	9	.	.	.	
	SEB-H02	200	6	150	100	6	9	156	150	9	
	SFB-H02	200	6	150	100	6	9	2Ls75	75	6	
SCB-H02	200	6	150	100	6	9	Ls 130	150	9		

(1 in=2.54 mm)

SDW- $\alpha \beta \gamma$ 

— Slab Concrete Strength 0 : none  
 — Filling Concrete Strength 1 : 29.4 MPa  
   2 : 17.7 MPa  
   3 : 23.5 MPa

— F : Filled with Concrete  
 H : Hollow  
 O : SHS not Connected

— Connection Model

SB : Simple Beam  
 SDW : Slender Hollow Section Direct Welded Joint  
 TDW : Thick Hollow Section Direct Welded Joint  
 SEB : Strong End Plate Bolted Joint  
 SFB : Short Fin Plate Bolted Joint  
 SCB : Seating Cleat Bolted Joint

### 3 Connection Tests

The tests were carried out in two stages. In the first stage, all the columns were

filled with concrete where the compressive strength was 29.4MPa(4.26ksi) and  $\phi 16$  mm( $\phi \frac{5}{8}$  in) reinforcing bars were arranged in one layer in 50mm(1.97in) spacing. In the second stage, some of columns were not filled and others were filled with concrete where the compressive strength was designed as 17.7MPa(2.56ksi) and 23.5MPa(3.41ksi) and the  $\phi 13$ mm( $\phi \frac{4}{8}$  in) steel bars were located in two layers with 50mm(1.97in) spacing.

### 3.1 Material properties

The coupons were cut out from the flat parts of the sections. Tensile fiat coupon test for steel sections and round coupon for reinforcing bars were carried out to obtain the yield and ultimate stresses and the elongation. Compressive mold tests were also executed to obtain material properties for the concrete and are given Table 2.2. The coupons were prepared and tested according to the Korean Standard KSB0801 and KSB0802 in a 250kN-Capacity testing machine. The nominal yield stress of steel sections and reinforcing bar are 240MPa(34.8ksi) and 400MPa(58.0ksi) respectively and ultimate tensile stress is 410MPa(59.5ksi) for the sections. As given in Table 2.1, the average yield and ultimate strength are much higher than the nominal strength due to the plastic deformation.

Table 2.1 Coupon Test Results

Specimen	t(mm)	$\sigma_y$ (MPa)	$\sigma_u$ (MPa)	Elongati on (%)
SHS Column	6	314.6(45.6) <sup>a</sup>	414.5(60.1) <sup>a</sup>	37.06
Beam Web	6	421.4(61.1)	549.8(79.7)	21.10
Beam Flange	9	296.9(43.1)	430.2(62.4)	21.10
Angle	6	319.9(46.9)	427.3(62.0)	20.83
Plate	8.6	340.1(49.3)	465.5(67.5)	40.10
Re-Bar	D16	453.7(65.8)	657.9(95.0)	25.04
	D13	594.9(86.3)	904.5(130.2)	22.05

(<sup>a</sup> in ksi)

Table 2.2 Concrete Mold Test Results

Test Stage	$F_c$ (MPa)	$\epsilon$ (%)	$E_c$ ( $\times 10^4$ MPa)	Slump (cm)
1 <sup>st</sup> Test	29.4(4.3) <sup>a</sup>	0.2	2.60(3770) <sup>a</sup>	7
2 <sup>nd</sup> Test	17.7(2.6)	0.2	2.01(2915)	7
	23.5(3.4)	0.2	2.32(3364)	7

(<sup>a</sup> in ksi)

### 3.2 Test results

Moment-rotation relationships were obtained using applied load  $P$  and displacement  $\Delta$  at center of the specimen. Since both ends of the specimen were simply supported, the moment and rotation of the flange of the column were computed as (Eq.1a &b)

$$M = \frac{P}{2} \left( \frac{L-B}{2} \right) \quad (1a)$$

$$\theta = \frac{\Delta}{(L-B)/2} \quad (1b)$$

where  $L, B$  was the beam length and the column width respectively. The test results of both stages are shown in Figs. 3.1 and 3.2.

A simply supported beam was tested for comparison with various connections. Initial stiffness, flexural rigidity and yield moment were obtained from the moment-rotation relationships. The classical method and beam-line theory were adopted to calculate the initial stiffness. In the classical method, the yield moment  $M_y$  is obtained at the intersection point of initial stiffness and parallel line with a third of initial stiffness as shown in Fig. 4 and rotation corresponding to the yield moment is  $\theta_y$ . The initial stiffness  $K_y$  is calculated as  $M_y/\theta_y$ . The results are given in Table 3. The increase of the thickness of the column does not make much difference in comparison between TDW-F11 and SDW-F11. The ratio of the yield moment, the ultimate moment, and the initial stiffness of the concrete filled column to the hollow column are shown in Table 4. From the results in the table, it is clear that filling concrete increase the flexural strength of the connections to a certain extent.

In 1990 Kishi and Chen proposed to use secant stiffness  $K_s$ , rather than initial tangent stiffness  $K_0$  which had been proven too high in real structural analysis. The secant stiffness is obtained at the point where vertical line from the intersection point of initial tangent stiffness and ultimate moment, and moment-rotation curve. Barakat and Chen proposed to use secant stiffness  $K_{sv}$  obtained from beam line theory in 1990. Beam line theory is given in (Eq. 2).

$$M_a = M_{Fa} + \frac{2EI}{L} \theta_a \quad (2)$$

In the single span beam, the end moment of the fixed boundary condition is  $M_{Fa}$  since  $\theta_a$  equals zero and the end rotation of simple boundary condition is  $-M_{Fa}/(2EI/L)$  since the end moment  $M_a$  equals zero. The secant stiffness is obtained at the intersection point of beam line and moment-rotation curve. The stiffness above mentioned are given in Table 5.

Table 3 Yield Moment and Initial Stiffness

Specimen		$M_y$ (k.Nm)	$\theta_y$ ( $10^{-3}$ rad)	$M_{max}$ (kN.m)	$\theta_{max}$ ( $\times 10^{-3}$ rad)	$\frac{M_{max}}{M_y}$	$K_y$	$_{SB}K_y$
1 <sup>st</sup> s t a g e	SB-001	10.25(7.6) <sup>a</sup>	9.33	15.35(11.3) <sup>a</sup>	58.25	1.50	1099	1
	SDW-F11	11.06(8.2)	12.47	15.04(11.1)	51.82	1.36	887	0.81
	TDW-F11	9.62(7.1)	10.44	13.71(10.1)	24.81	1.43	921	0.84
	SFB-F11	8.34(6.2)	21.72	14.62(10.8)	84.42	1.75	384	0.35
	SCB-F11	13.54(10.0)	19.65	16.81(12.4)	38.35	1.24	689	0.63
2 <sup>nd</sup> s t a g e	SB-002	11.25(8.3)	11.30	12.78(9.4)	28.12	1.21	995	1
	SDW-F22	9.68(7.1)	11.42	12.58(9.3)	41.92	1.30	848	0.85
	SEB-F22	8.16(6.0)	9.15	13.49(9.9)	87.21	1.65	892	0.90
	SFB-F22	5.08(3.7)	13.84	12.34(9.1)	85.24	2.43	367	0.37
	SCB-F22	12.61(9.3)	20.02	17.41(12.8)	64.52	1.38	630	0.63
	SDW-F32	10.70(7.9)	12.20	15.02(11.1)	67.50	1.41	877	0.88
	SEB-H02	4.80(3.5)	13.62	6.53(4.8)	90.62	1.36	352	0.35
	SFB-H02	3.20(2.4)	12.44	5.12(3.8)	93.94	1.60	257	0.26
	SCB-H02	5.94(3.7)	15.50	7.95(5.2)	50.51	1.34	383	0.38

$M_y$  : yield moment,  $M_{max}$  : maximum moment (<sup>a</sup> in ksi)

$\theta_y$  : rotation at yield,  $\theta_{max}$  : maximum rotation,

$K_y = M_y/\theta_y$  : initial stiffness

Table 4 Comparison between Concrete Filled and Hollow SHS column

Specimen	$F M_y / H M_y$	$F M_{max} / H M_{max}$	$F K_i / H K_i$
SEB-F22(-H02)	1.7	2.07	2.53
SFB-F22(-H02)	1.59	2.41	1.43
SCB-F22(-H02)	2.12	2.19	1.58

F, H indicate filled and hollow respectively.

The ratio of each stiffness to that of simply supported beam is also shown for

comparison. The initial stiffness  $K_0$  ranges from 93% to 23% of that of simple beam. In the first test,  $K_0$  is higher than  $K_{si}$  by 34% and than  $K_{sv}$  by about 5% and  $K_{sv}$  is higher than  $K_{si}$  by 29%.

Table 5 Flexural Rigidity of Connections

Specimen		Flexural Rigidity [MN.m/rad]			Ratio to SB		
		$k_0$	$k_{si}$	$k_{sv}$	$k_0/k_0(SB)$	$k_{si}/k_0(SB)$	$k_{sv}/k_0(SB)$
1 <sup>st</sup> s t a g e	SB-001	19.19	.	.	.	.	.
	SDW-F11	11.39	8.48	10.86	0.59	0.44	0.57
	TDW-F11	11.82	8.85	11.14	0.62	0.46	0.58
	SFB-F11	52.4	3.49	5.09	0.27	0.18	0.27
	SCB-F11	78.2	6.65	7.47	0.41	0.35	0.39
2 <sup>nd</sup> s t a g e	SB-002	17.04	.	.	.	.	.
	SDW-F22	13.98	8.89	12.75	0.82	0.52	0.75
	SEB-F22	11.34	7.48	11.16	0.67	0.44	0.65
	SFB-F22	4.98	2.61	4.25	0.29	0.15	0.25
	SCB-F22	10.75	6.85	7.54	0.63	0.40	0.44
	SDW-F32	15.81	10.21	13.95	0.93	0.60	0.82
	SEB-H02	52.2	3.62	4.22	0.31	0.21	0.23
	SFB-H02	39.4	2.46	2.84	0.23	0.14	0.17
SCB-H02	54.8	4.10	4.65	0.32	0.24	0.27	

From the second test result, it is shown that the initial stiffness  $K_0$  is higher than  $K_{si}$  by 58% and than  $K_{sv}$  by about 22% and  $K_{sv}$  is higher than  $K_{si}$  by 33%, which is much higher when compared with the first test results. The comparison between the results obtained by two different methods shows big difference. Generally, in the first test, initial stiffness  $K$  is higher than  $K_{si}$  by 4–10% and than  $K_{sv}$  by 8–33% and in the second test,  $K$  is higher in some specimen and lower in other specimen than  $K_{si}$  by 3–40% and  $K_{sv}$  is higher than  $K$  by 10–60%. It seems to be very difficult to find a general rule or a trend for the rotational stiffness of connections obtained by two different methods.

### 3.3 Flexural rigidity for connections

CIDECT(1986) made a provision for the deformation limit of the flange of the tubular sections as  $b_c/100$ . In this research, the limit rotation of the flange can be estimated approximately when the horizontal deformation reaches the limit. Since the width of the column is 200mm and the depth of beam is 150mm, the rotation should range from 2/75 to 2/150. In this paper, the critical rotation is assumed as 2/100 radian and the corresponding yield moment and the maximum moment are compared



in Table 6. The results show that the ratio to simple beam(SB) ranges from 33% to 100%. For the yield moment, concrete filling increase the ratio from 14%(SFB) up to 43%(SCB) and approximate 30% is enhanced for the average value.

Table 6 Yield and Ultimate Moment Compared with Simple Beam

Specimen	Moment [kN.m]		Ratio to SB	
	yield moment	ultimate moment	yield moment	ultimate moment
SB-001	137(10.1) <sup>a</sup>	153(11.3) <sup>a</sup>	1.0	1.0
SDW-F11	136(10.1)	150(11.1)	0.994	0.980
TDW-F11	134(9.9)	137(10.1)	0.977	0.893
SFB-F11	77(5.7)	146(10.8)	0.565	0.952
SCB-F11	136(10.0)	168(12.4)	0.991	1.095
SB-002	127(9.4)	127(9.4)	1	1
SDW-F22	119(8.7)	125(9.3)	0.930	0.984
SEB-F22	102(7.5)	134(9.9)	0.801	1.055
SFB-F22	59(4.4)	123(9.1)	0.469	0.966
SCB-F22	126(9.3)	174(12.8)	0.990	1.362
SDW-F32	129(9.6)	150(11.1)	1.019	1.175
SEB-H02	56(4.2)	65(4.8)	0.443	0.511
SFB-H02	41(3.1)	51(3.8)	0.325	0.401
SCB-H02	69(5.1)	79(5.9)	0.544	0.622

(<sup>a</sup>in ksi)

AISC Specifications(1989 ASD) has provisions for the connections where the connections are divided in three categories such as rigid, semi rigid and simple connections according to the extent of restraint. The ratio of the moment of connections obtained by beam line method to fixed end moment of simple span beam is used for division. The results are given in Fig. 6. The rigidity ratio for the test specimen are ranged from 35% to 95%. Specimens SDW-F11, TDW-F11 and SDW-F32 has more than 90% and can be regarded as a rigid connection. All the others are assumed as a semi rigid connection since the values are between 20% and 90%. Generally the flexural rigidity of the connections tested seems to be quite enough to resist the applied load if designed properly.

#### 4 Structural Analysis for Connections

##### 4.1 Numerical simulations using FEM

The structural behavior of the connections were analyzed using inelastic nonlinear finite element procedures(ADINA 1987) and were compared with the test results in

Figs. 7.1-7.3. The results are agreed quite well for the moments. The difference is about 2-9% for the yield moment and 1-6% for the ultimate moment. However, the initial stiffness calculated numerically is around 30% higher than that of the test results. The difference may be mainly due to concrete cracks occurred at the loading stage which can not be considered properly in the numerical analysis. Therefore, the advanced technique to trace nonlinear behavior of the composite connections in tri-axial status should be developed to produce more accurate initial flexural stiffness.

#### 4.2 Proposed power model

The power model for bolted connections which was proposed by Colson and Louveau(1983), and Kishi and Chen(1990) and modified to apply for the welded connections by the author(1995) were applied to the connections between composite SHS column and W-section beams. The proposed model is of the form

$$\theta = \frac{M}{K_i} \frac{1}{[1 - (M/M_u)^{\frac{n}{m}}]^{\frac{1}{n}}} \quad (3)$$

in which  $K_i$  is the initial flexural stiffness,  $M_u$  is the ultimate moment capacity of the connections (flat part of the moment-rotation curve) and  $m, n$  are shape parameters. The expected results are compared with the test results in Fig. 8 with different  $m, n$  values. The initial stiffness expected is well agreeable with the test result but the ultimate stress is slightly lower than the test result.

#### 5. Conclusions

In this paper, the semi-rigid connection, which is composed of concrete filled SHS columns and composite beams, was studied for the application in construction of the multi-story buildings. Several connection models were tested and compared with the numerical results.

The thickness of the SHS columns filled with concrete has little effect on the initial flexural stiffness of the connections. Therefore, width to thickness ratio should be studied more to recommend an optimum limit. The in-filled concrete has a considerable effect on the rigidity of the connections since it resists against compressive force transferred. The concrete compressive strength has an effect on the yield moment of the connections at the limit deformation. The connections filled with the high strength concrete moves closer to the rigid connection limit.

End plate connections of the concrete filled columns have much higher flexural rigidity than those of hollow columns. Fin plate connections are similar to the simple type regardless of the filling concrete. Bottom seat cleat connections are useful in both ways of rigidity and fabrication, which can be recommended for the semi-rigid connection of the tubular section columns used for the multi-story buildings.

## 6. References

- ADINA(1987); A Finite Element Program for Automatic Dynamic Incremental Nonlinear Analysis, Report ARD87-1, ADINA R&D, Inc..
- AISC Specification for Structural Steel Buildings(1989); Allowable Stress Design and Plastic Design with Commentary.
- Barakat, M. A. and Chen, W. F. (1989); Practical Analysis of Semi-rigid Frames, Engineering Journal, AISC, 27(2), pp54-68.
- CIDECT(1986); Comite International pour le Development et l'etude de la Construction Tubulaire, "The Strength and Behaviour of Statically Loaded Welded Connections in Structural Hollow Sections", CIDECT Monograph No.6.
- Colson, A. and Louveau, J. M. (1983); "Connections Incidence on the Inelastic Behavior of Steel Structures", Euromech Colloquium174.
- Ji, H. L., Kanatani and Tabuchi, M.(1989); "Behavior of Concrete Filled RHS Column to HT-Bolts", proceedings, International Symposium on the Tubular Structures, pp196-203.
- Jung, H. C., Lee, J. S. and Kwon, Y. B. (1995); "A Study on the Behavior of the Connections between SHS Column and W-section Beams", proceedings, Fifth East Asia-Pacific Conference on Structural Engineering and Constructions. pp737-743.
- Kishi, N and Chen, W. F. (1990); "Moment Rotation Relations of Semi-rigid Connections with Angles", J. of Structural Engineering, ASCE, 116(7), pp1813-1834.
- Morita, K et al. (1992); "Experimental Study on Connections Between Concrete Filled Square Tubular High Strength Steel Column and H-Beam", Proceedings, Third PSSC, Tokyo, Japan.

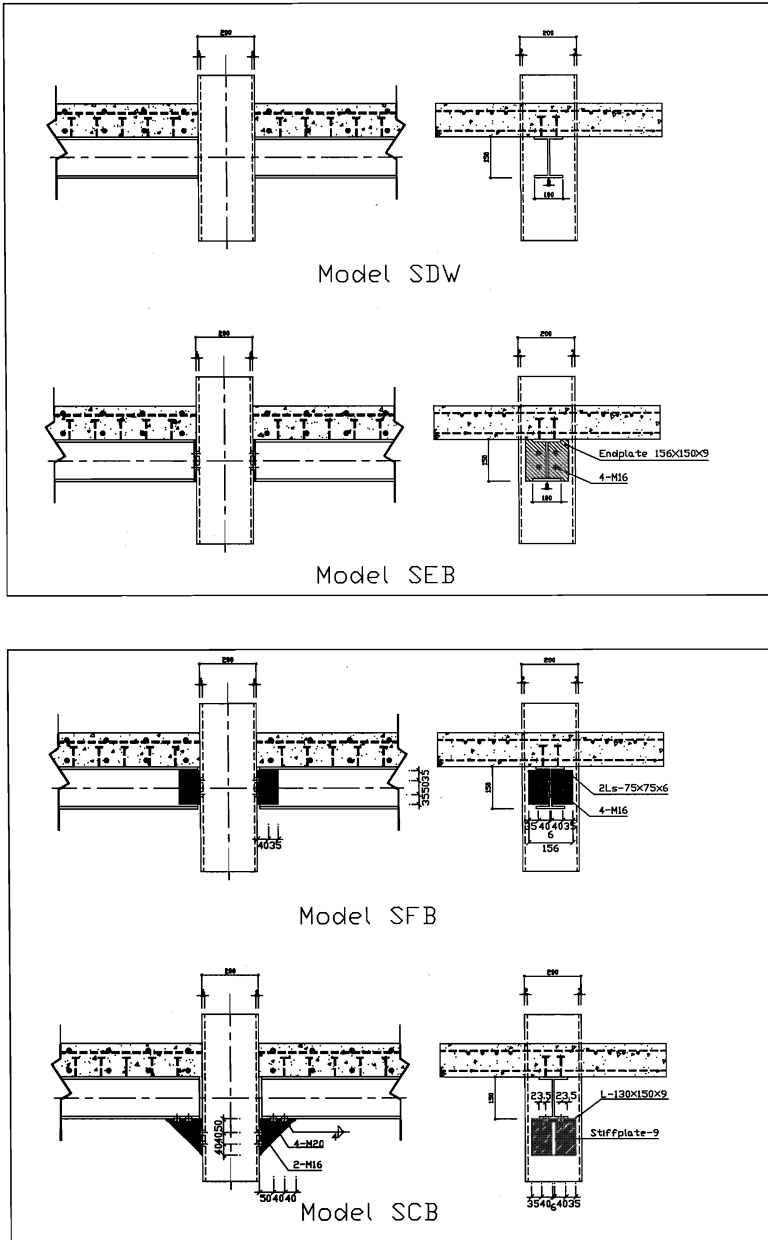


Fig. 1 Connection Types

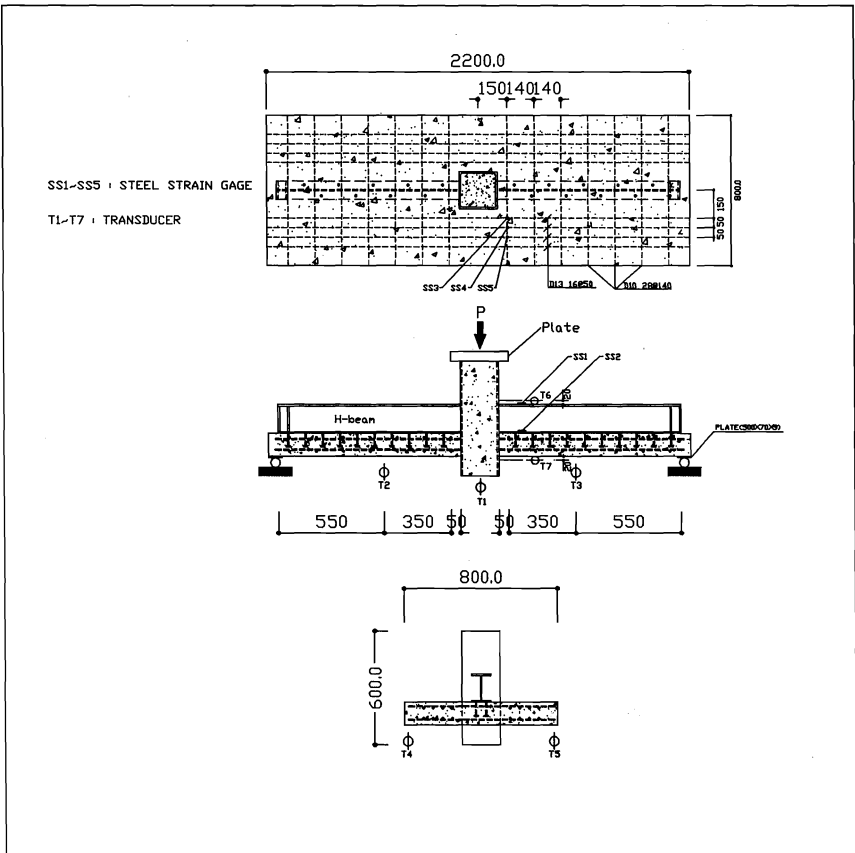


Fig. 2 Layout of Connection Test

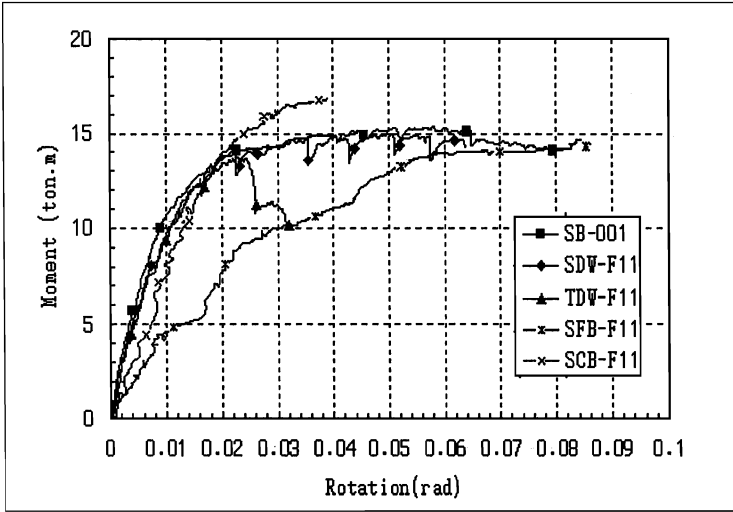


Fig. 3.1 Moment versus Rotation for 1st Tests

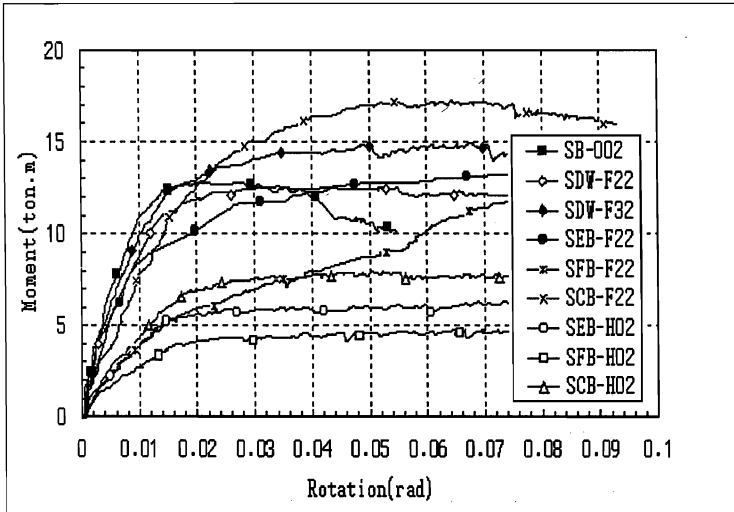


Fig. 3.2 Moment versus Rotation for 2nd Tests

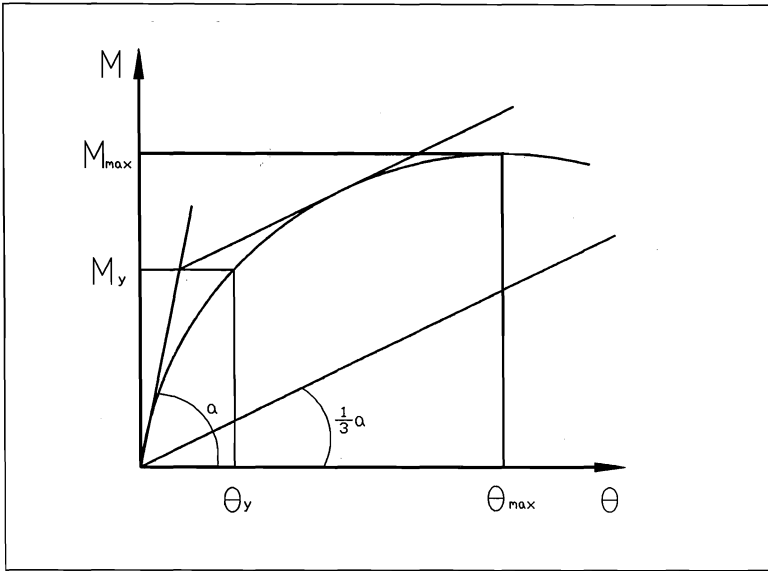


Fig. 4 Classical Method for the Design Stiffness

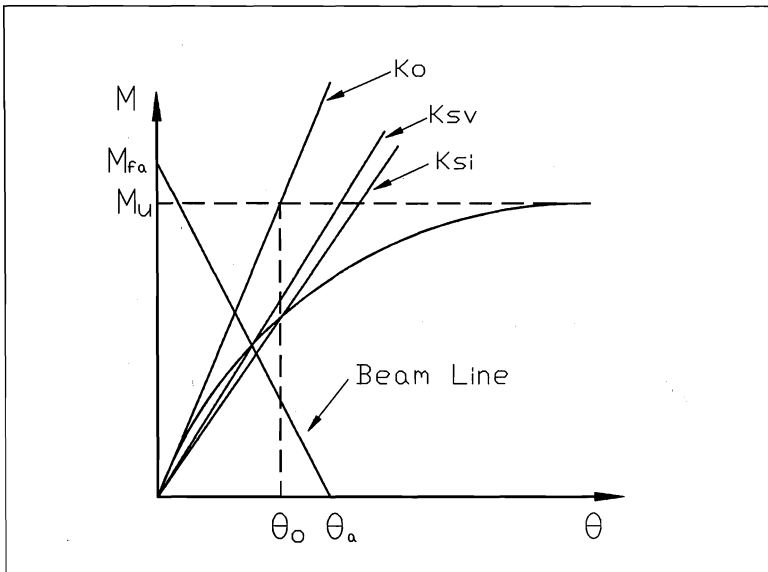


Fig. 5 Beam-Line Method for the Design Stiffness

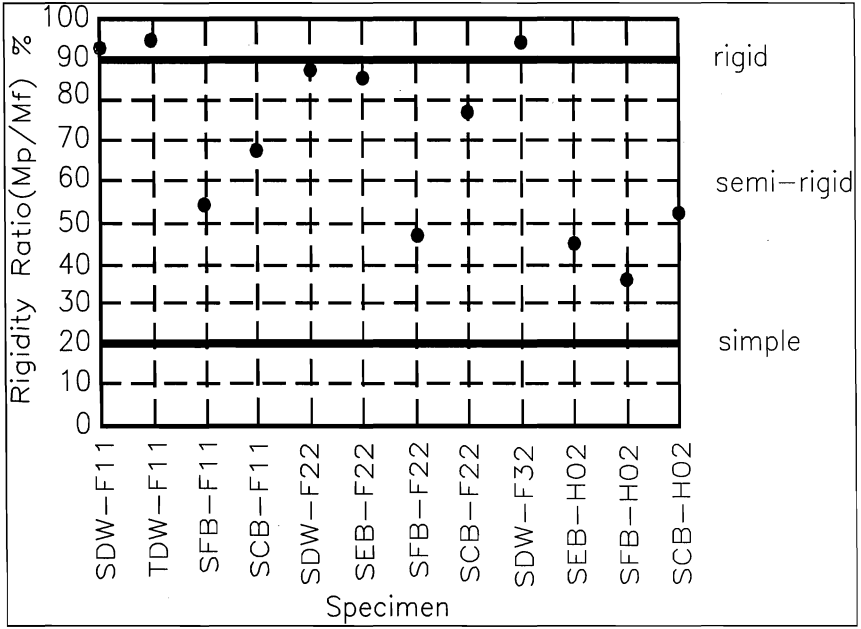


Fig. 6 Connection Rigidity acc. to AISC



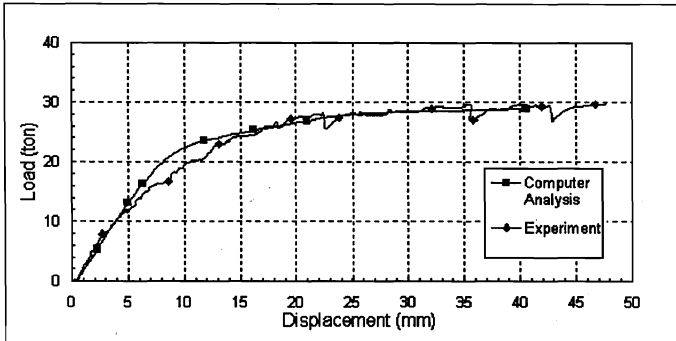


Fig. 7.1 Comparison between Numerical and Test Results(SDW)

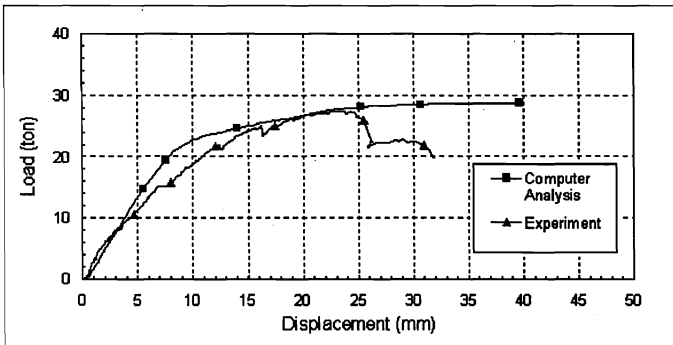


Fig. 7.2 Comparison between Numerical and Test Results(TDW)

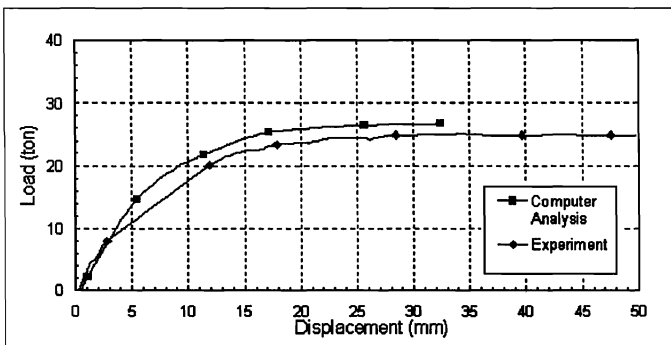


Fig. 7.3 Comparison between Numerical and Test Results(SDW2)

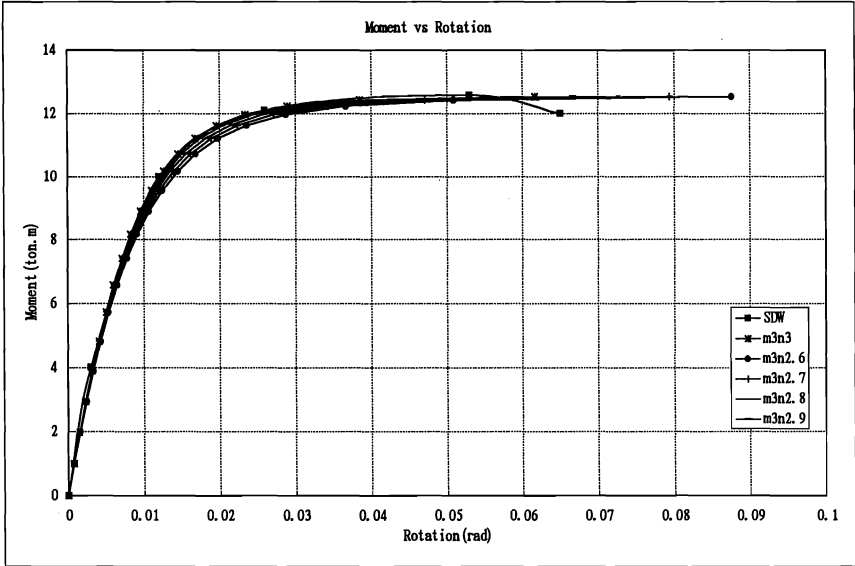


Fig. 8.1 Comparison between Power Model and Test Results ( $m=3$ )

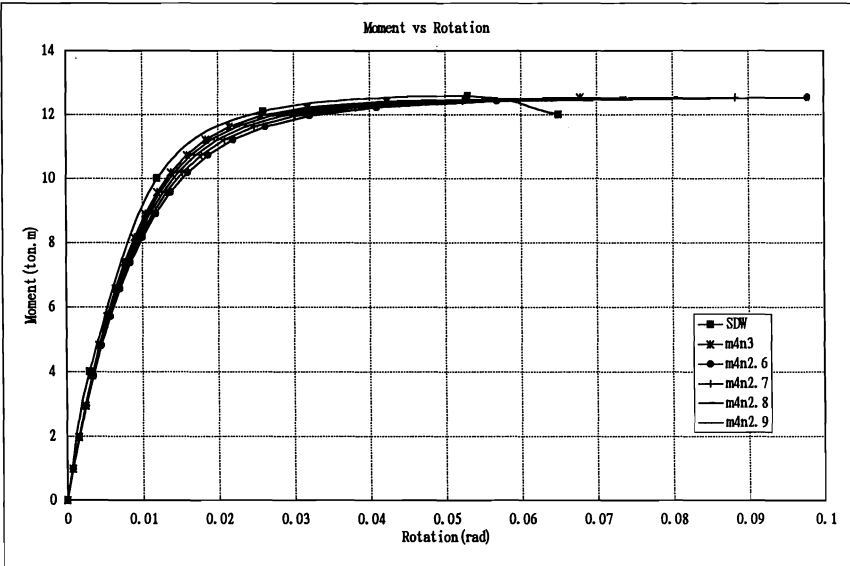


Fig. 8.2 Comparison between Power Model and Test Results ( $m=4$ )

